DOI: 10.5505/2023geoteknik.SS-22

INVESTIGATING THE EFFECTS OF LATERAL DEFORMATIONS IN CPS EMBANKMENTS ON SOIL ARCHING: A PARAMETRIC STUDY USING FINITE ELEMENT ANALYSIS

KAZIKLARLA DESTEKLENMIŞ GELENEKSEL DOLGULARDA KEMERLENME MEKANIZMASI ÜZERINDE YATAY DEFORMASYONLARIN ETKISI: SONLU ELEMANLAR YÖNTEMI ILE PARAMETRIK ARAŞTIRMA

Araz Salimnezhad[1], Mostafa Almasraf[2]
Safiye Feyza Cinicioglu[3], Ozer Cinicioglu[4]

ABSTRACT

The behavior and design of piled embankments constructed on soft soils are significantly influenced by soil arching, characterized by the redistribution of stresses between the yielding mass and the surrounding non-yielding soil. On the other hand, lateral spreading action within the embankment acts as another factor that influences the load distribution mechanism. Paying attention to the role of lateral deformations and stress axis rotation, this study investigated arching behavior in piled embankments under self-weight using nine FEM analyses under plane strain conditions. A series of Plaxis models were employed to examine the impact of geometry parameters such as embankment height and center-to-center pile spacing on arching evolution. The lateral earth pressure coefficients and horizontal deformations inside the fill were utilized to understand the center, shoulder, and toe arch formation mechanism. The results indicate that the lateral earth pressure coefficient can be a logical indicator of soil arching.
Keywords: *Soil arching, piled embankments; principal stress directions, lateral earth pressure coefficient, horizontal deformation*

1. INTRODUCTION

Transportation systems play a critical role in modern societies, covering large distances and requiring unique considerations for their design. In particular, soil-structure interaction is a crucial factor in the design of transportation structures such as embankments, tunnels, and pipelines. Embankments are commonly built in lowland areas with soft and alluvial soils, making them susceptible to significant settlements and deformations. To address these challenges, two common approaches are used: controlled stage construction techniques (Indraratna et al. 2005, Oztoprak and Cinicioğlu 2005, Oser and Cinicioglu 2017) or embedding piles into the soft soil beneath the embankment (Han and Gabr 2002, Kelesoglu and Cinicioğlu 2010). The latter approach can facilitate soil arching, a phenomenon resulting from soil-structure interaction that has garnered academic interest in recent decades. Several studies have explored the economic and optimal use of piles beneath embankments and their potential to enhance soil arching. Nevertheless, the stability and durability of the load transfer system, which arise from arching, continue to be areas of ongoing research and demand further investigation (Van Eekelen et al. 2013, King et al. 2017).

Embankments supported by piles or containing high modulus columns are commonly referred to as "conventional pile-supported (CPS) embankments." CPS embankments are more efficient than the embankments built using the staged construction approaches as they can significantly reduce anticipated

[1] Department of Civil Engineering, Ozyegin University, Istanbul, Turkey, araz.salimnezhad@ozu.edu.tr
[2] Department of Civil Engineering, Ozyegin University, Istanbul, Turkey, mostafa.almasraf@ozyegin.edu.tr
[3] Department of Civil Engineering, Ozyegin University, Istanbul, Turkey, feyza.cinicioglu@ozyegin.edu.tr
[4] Department of Civil Engineering, Bogazici University, Istanbul, Turkey, ozer.cinicioglu@boun.edu.tr

settlement and shorten the construction duration (Mesri and Choi 1985, Mesri et al. 1994, Fagundes et al. 2017, King et al. 2017). Additionally, CPS embankments can prevent local failure and deformation (Van Eekelen et al. 2020). In these systems, the load from the fill material is primarily transferred to the piles through the arching mechanism established in the granular fill, with only a minimal portion of the load being carried by the underlying soft soil (Hewlett and Randolph 1988, Van Eekelen et al. 2013). The arching mechanism plays a vital role in governing the behavior of these structures as it controls the stress distribution between soil and structural elements with different rigidities. Soil arching occurs due to the relative displacement of piles and soil. CPS embankment design and performance rely heavily on the arching mechanism, and several factors can impact the stability and performance of these formations (Rui et al. 2019).

In accordance with the Hewlett and Randolph (1988) model, the lateral earth pressure coefficient (k) can be categorized into three states within the arched zone between two piles. These K values correspond to the active, passive, and at-rest states for the points above the pile, above the subsoil, and above the equal settlement plane, respectively. Examining the variation of K values in both the horizontal and vertical directions inside the fill can effectively monitor the arching behavior and its geometry. Moreover, K values can provide a valuable means of interpreting pile efficiency and avoiding misinterpretation of evidence related to arching formation. Prior research on the behavior of CPS embankments has primarily focused on modeling specific sections of the embankments, typically the span between the centerlines of mid-piles, while assuming horizontally rigid side boundaries. Physical and numerical models, such as single or multi-trapdoor models, developed to investigate arching behavior were also restricted by horizontally constrained rigid side walls. Therefore, the effect of the embankment's lateral spreading (deformation) on soil arching and its behavior has been overlooked. Moreover, the piles located at the sides of embankments undergo considerable lateral deformation, resulting in a different arching behavior and consequently affecting the transfer of loads to the piles.
This study investigates the potential interrelationships between piles layout, embankment heights, horizontal displacement of the fill, piles' deflection, lateral earth pressure coefficient value, and arching evolution through parametric 2D finite element analyses. The parametric study comprises different embankment heights and pile spacings constructed over a specific soil profile. For this purpose, nine Plaxis 2D model tests were conducted, and the results are presented in this paper.

2. MAIN FEATURES OF THE PARAMETRICAL ANALYSES

The conventional pile-supported (CPS) embankment under self-weight in a plane strain 2D condition was modeled using the finite element method (FEM) based software Plaxis 2D Ultimate. The soil profile of Stanstead Abbots (Willow Plantation or Harlow) was selected as a well-documented case history to represent the soft ground over which the embankment will be constructed (Oztoprak and Cinicioglu 2007, Hird et al. 1995). The Stanstead Abbotts embankment was constructed in 1988 on very soft alluvial deposits with a height of 8.05 m in 274 days. The soil stratigraphy and geotechnical properties of Stanstead Abbotts are presented in Fig. 1 and Table 1, respectively. The groundwater table is located at a depth of 1.5 m beneath the ground surface. To focus on the arching behavior, the embankment's shoulder slopes were defined as 1:3 (V: H) to prevent potential slope instability.

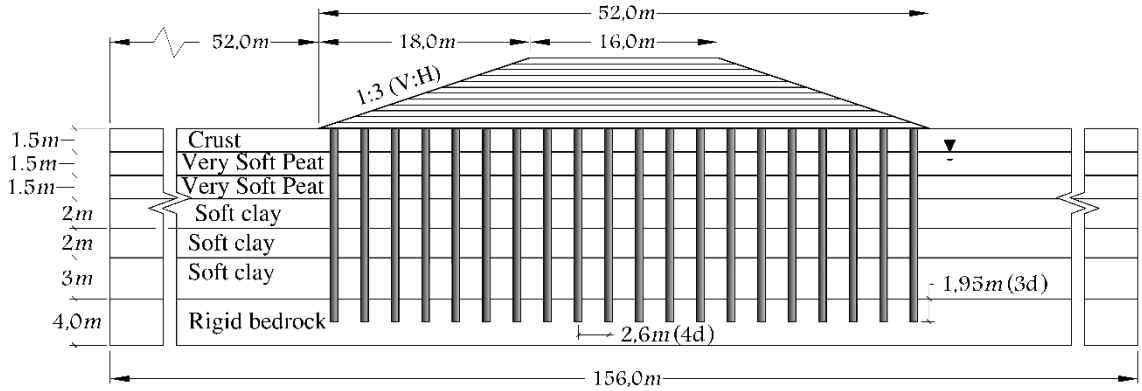

Figure 1. Considered embankment model.

The behavior of the soft ground beneath the embankment was modeled using the Soft Soil model with undrained loading stages followed by the consolidation stages in between. This model was found to be appropriate for simulating the settlement behavior of the soft peat and clay layers, which undergo consolidation in the presence of groundwater at a depth of 1.5m. The soft soil model is based on the Cam-Clay model and is particularly well-suited for modeling near-normally consolidated clays, silty clays, and peat, especially during primary compression scenarios. Changes in void ratio and therewith, in soil permeability during the consolidation process were considered using the void ratio dependency factor C_k = 0.5 e_0 and defined as log k = log k_0 – ((e_0 – e)/C_k), where k_0 and e_0 represent the initial values of permeability and void ratio, respectively (Taylor 1948, Tavenas et al. 1983).,

The Modified swelling and compression indices defined as $\lambda^* = \lambda/(1+e)$ and $k^* = k/(1+e)$ are used in the Soft Soil model and differ from their original Cam-Clay counterparts, described by Burland (1965) as the modified parameters are a function of volumetric strain rather than the void ratio. Three different heights (6, 8, and 10m) were considered to analyze the behavior of the piled embankments resting on the considered soil profile. Stage construction technique was adopted, and sublayer thicknesses were chosen as 0.5m. After completion of the embankment construction, a final consolidation phase was allowed to let excess pore pressure dissipate.

Table 1. Material parameters for the piled embankment.

Material	Soil Model	Unit weight		Poisson's ratio	Permeability	Void ratio	Adopted from Hird et al., 1993		
		γ_{unsat} (kN/m^3)	γ_{sat} (kN/m^3)	ν_{ur}	$K_x=k_y$ (m/s)	e_0	λ^*	κ^*	ϕ' (°)
Crust	Soft Soil	13	16	0.15	2.5×10^{-5}	0.8	0.060	0.009	29
Very soft peat		7.4	11.4	0.15	2.5×10^{-5}	7.3	0.147	0.006	34
Very soft peat		7.4	11.4	0.15	2.5×10^{-5}	8.2	0.179	0.020	34
Soft clay		13.2	16.2	0.15	2.5×10^{-10}	1.5	0.163	0.015	28
Soft clay		13.2	16.2	0.15	2.5×10^{-10}	1.45	0.158	0.013	28
Soft clay		13.2	16.2	0.15	2.5×10^{-10}	1.4	0.060	0.009	28
Embankment fill	Hardening Soil	16	19	0.2	4×10^{-5}	0.5	E_{50}^{ref} (kN/m^2)	E_{oed}^{ref} (kN/m^2)	E_{ur}^{ref} (kN/m^2)
							25×10^3	25×10^3	75×10^3
Bedrock	Mohr-Coulomb	27	30	0.3	-	0.5	E'_{ref} (kN/m^2)	-	-
							4.9×10^6		
Pile	Linear Elastic	24	24	0.3	-	-	30×10^6	-	-

Consolidation proceeded until almost a full dissipation of the excess pore pressure state was reached, and the termination value was selected as 1 kN/m^2 for the excess porewater pressure. A reduction factor (R_{inter}) of $2/3\phi'$ was applied on the shear strength angle of the soil surrounding the piles to define the interaction in the soil-structure system (Karthigeyan et al. 2007, Zheng et al. 2019, Jenck et al. 2007). A bedrock layer with a thickness of 3.95 m was placed at the bottom of the soft soil layers. The piles of 13.45 meters were considered to embed for a depth of 3d into the bedrock. The pile diameters (d) were taken as 0.65m across all models. The center-to-center spacing of the piles varied as 4d, 5d, and 6d (Table 1).

3. RESULTS AND DISCUSSION

Figure 2a displays the variation in K values against the fill height through a vertical cross-section from the top to the bottom of the embankment centerline for a 4d pile spacing. The K value is 0.33 between the top of the embankment and 3.5m above the subsoil, which represents the critical active condition within this range. The active condition is controlling the behavior between 3.5m to 2.25m above the piles, while the fill is in a passive condition under a height of 2.25m above the subsoil. For the 8H-4d case, the K value is K_p=3 at a height of 0.8m above the subsoil, based on an internal friction angle of 30° for the fill material. Irrespective of fill height, the highest K value (greatest compression) for the 4d case lies in the 0.5m to 0.8m range above the subsoil.

The variation in K values with respect to the fill height through a vertical cross-section from the top to the bottom of the embankment fill centerline for the 5d pile spacing is depicted in Figure 2b. The K value is 0.33 between the top of the embankment and 4m above the subsoil, representing K_a in this range. For all heights in the 5d spacing, the K value almost reached the critical K_p=3 at a height of 0.75m for 6m, and 10m fill heights, and at 1m above the subsoil for an 8m fill height. Under a height of approximately 3m above the subsoil, the fill is in a passive condition.

Figure 2c illustrates the variation in K values with respect to the fill height through a vertical cross-section from the top to the bottom of the embankment fill centerline for a 6d pile spacing. The K value is 0.33 between the top of the embankment and 4.5m above the subsoil, representing Ka in this range. For all heights in the 6d spacing, the K value almost reached the critical K_p=3 in the range of 0.8m to 1.2m above the subsoil. Under a height of approximately 3.5m above the subsoil, the fill is in a passive condition (K_p >K> K_0).
The passive region (compression) is a key indicator of arching and mobilized shear strength. The thickness of the passive region increases with the increase of pile spacing. Therefore, increasing pile spacing for the same fill height will result in the arched shear bands (or force chains) reaching a higher height above the subsoil. However, the strongest part of the formed arches is located where the K value is closest to K_p, indicating the greatest compression of the soil grains.

Previous studies using trapdoor models or specific embankment sections have shown that, due to the rigidity of the side walls or boundaries, the K values through the same vertical cross-section start from K_0=0.5 and reach K_p in the arching zone (Meena et al., 2020). This behavior is due to the limited horizontal deformation of soil in models with rigid side boundaries. In contrast, modeling the full-size embankment allows for lateral spreading of the fill from the centerline towards the sides, resulting in the formation of the active zone under the crest. The height above the subsoil that the arches reach their strongest mode (the greatest compression) increases with the increase of the pile spacing. This observed behavior is consistent with the Hewlett and Randolph (1988) model.

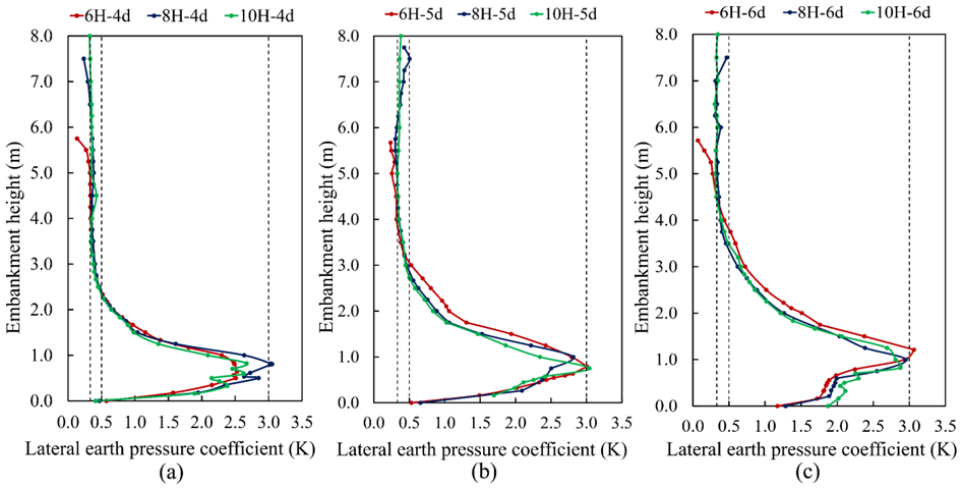

Figure 2. Lateral earth pressure at the embankment centerline for different heights for: a. 4d spacing; 5d spacing; 6d spacing.

Figure 3a illustrates the variation of the K value throughout the horizontal cross-sections in the right half of the 8H-4d embankment, extending from the centerline to the shoulder slope, at heights of 0.5, 1, 1.5, 2, 2.5, and 3m above the sub-soil. The figure also shows the change in the K value across the horizontal cross-section at the base of the 8m high embankment with no piles, and the location of the piles is included to aid in tracking the K values' alteration. The K values were averaged for the 0.5m high horizontal cross-section above the subsoil span. As shown in the 0.5m high cross-section, the K values almost reach the critical K_p=3 value at the central parts of the fill, indicating strong compression and a stable arch structure. However, the K value decreases towards the toe to almost half the K_p on the same cross-section. The K value on the pile heads is also noteworthy, being equal to Ka=0.33 (active condition), indicating the punching of the piles into the embankment base. With an increase in the height of the horizontal cross-sections, the K value decreases due to the increased distance from the subsoil vertically, resulting in the K value being equal to K_a=0.33 at a height of 3m above the subsoil in the central part of the fill, indicating the decompression and degradation of the arches.

The K value variation for the non-piled 8m high embankment at the fill base exhibits that up to a 13m distance from the embankment centerline in the horizontal direction, the K value is almost identical to K_a, but beyond that point, the K value begins to increase (up to 2) as it approaches the toe. The absence of any high modulus structural element eliminates arching as a possible cause for the increased K value. Rather, the main reason for the increased K value is the inclined nature of the loads at the sloped part under the fill's shoulders. This is due to the fact that the magnitude of the vertical stress along the embankment base decreases from the centerline up to the toe, while the magnitude of the horizontal stress of the non-piled 8H embankment rises, moving from the centerline towards the toe. Over the range of 13.5m from the centerline, the horizontal stress is nearly constant at approximately 40 kN/m^2, and from 13m to 22m, this value grows to a peak of 95.5 kN/m^2, before decreasing steadily to 0 kN/m^2 at the edge of the toe. Consequently, the K value's increasing trend for the 8H-4d embankment along the horizontal cross-sections from the center towards the toe at a height beyond 1m is not exclusively due to arching, and the inclination of the fill shoulders has a much greater impact.

Figure 3b illustrates the total horizontal displacement values of the 8m high embankment at the base level for the piled (4d spacing) and non-piled cases. In the non-piled embankment, the displacement is negligible at the center, but it increases to a maximum value of 0.56m at a distance of 16.5m from the center and remains almost constant thereafter. In contrast, the model supported with piles shows significantly smaller horizontal displacement values, with a maximum of 0.04m (14 times smaller) due to the presence of high modulus elements (piles). The horizontal displacement trend of the piled embankment differs from the non-piled model. For the piled embankment, the horizontal displacement increases up to a distance of 17.5m from the center and remains constant (0.04m) up to a distance of 21.5m from the center before reaching a value of 0.016m over the last pile. The distance from the center at which the horizontal displacement starts to decrease from the maximum value is nearly the same as the onset point distance for horizontal stress reduction.

Figure 3c displays the principal stress direction and geometry of the arch structures formed at three locations along an 8m high embankment base with 4d pile spacing. The three locations are the center, mid-half, and toe of the embankment base and are labeled 1, 2, and 3, respectively. At the center of the fill, the principal stresses above the subsoil indicate a rotation to a horizontal state at a specific height above the subsoil centerline, forming an arched area that carries the burden of the fill portion above the arch structure. The arch has a symmetrical geometry, as indicated by the dashed lines representing shear bands emanating from the corners of the center piles (Figure 3-c1).
In the mid-half region, which almost coincides with the middle of the inclined fill shoulder, the inclined nature of the soil loads causes the directions of the principal stress to be not aligned vertically above the arching zone. As a result, the angle between the shear band trajectories (arch legs) with the pile heads is not equal for two consecutive piles, resulting in an asymmetrical parabolic geometry of the formed arch structure (Figure 3-c2).

In the span close to the toe, the principal stress directions are almost parallel to the slope of the inclined fill shoulders, resulting in ineffective overlapping to form an arch. Due to the low fill height at the toe part, the

arching was not fully mobilized, and the arch did not carry a noticeable burden (Figure 3-c3). The trajectory of the principal stress directions suggests that the arches extended to the fill surface.

Figure 3d shows the lateral deflection of piles at head level versus their distance from the centerline of the 8m high embankment for various pile spacing values. The pile deflection behavior was similar for all models, starting from approximately zero at the center, rising to a peak value under the middle of the inclined shoulder, and falling to a final value at the edge. The lateral deflection of piles reached its maximum value at a distance of 20m from the centerline and increasing the pile spacing resulted in higher pile deflection. The peak value of pile lateral deformation for 4d, 5d, and 6d cases was determined to be 2.8cm, 4.4cm, and 5.7cm, respectively.

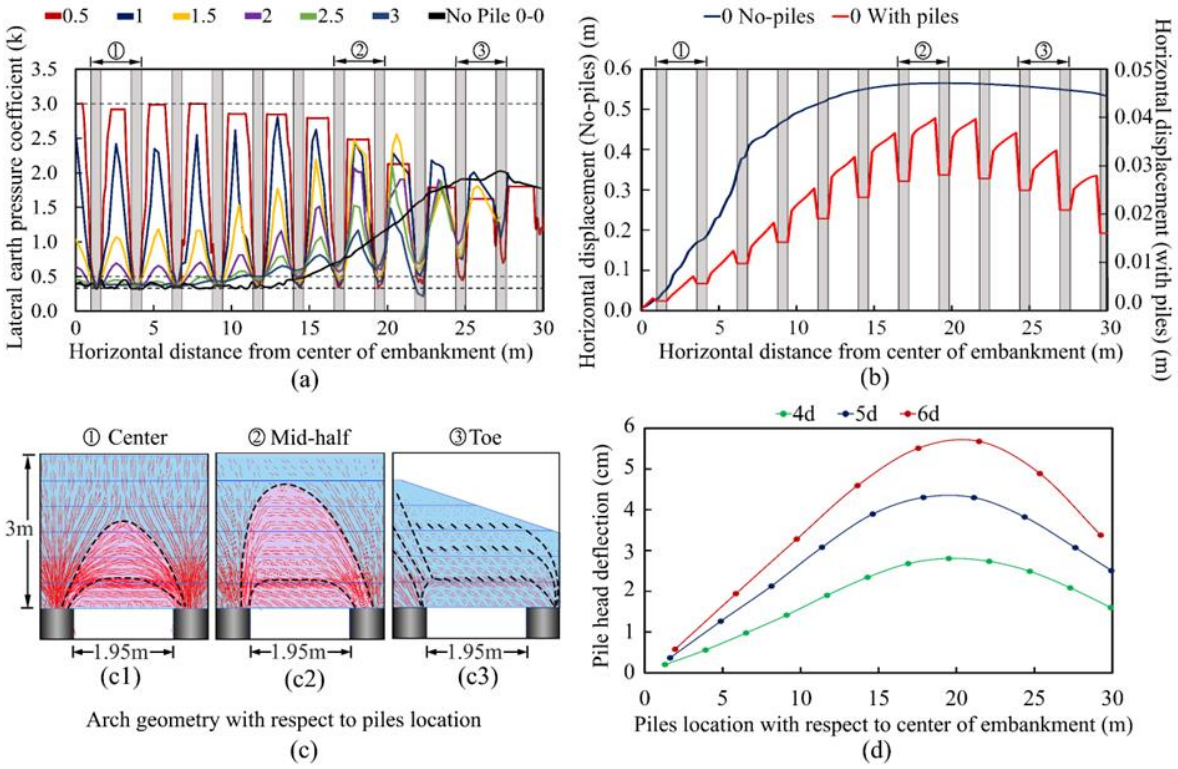

Figure 3. Numerical analyses results of (8m H-4d) embankment for: a. Lateral earth pressure along the embankment's half-length; b. Horizontal displacement of the embankment base; c. Principal stress directions for different pile location; d. Pile head deflection for different pile spacing.

Comparing and analyzing the geometries of various arch structures, it was noted that the height of the mid-half arch is greater than that of the central full arch, which agrees with the findings reported by Lai et al. (2018). Based on the observed changes in arch geometry depicted in Fig. 3c, it can be hypothesized that the reason for such variations is the dependence of arch geometry on the stress state. Higher levels of stress lead to more compact arch geometries.

4. CONCLUSIONS

This study presents a numerical investigation on the behavior of pile-supported embankments under plane strain conditions, focusing on soil arching. The study utilizes the Soft Soil model for soil layers beneath the embankment and Hardening Soil model to examine the evolution of soil arching. A parametric study is conducted to investigate the effects of varying parameters, such as pile spacing and embankment height, on the mechanism of soil arching formation. Based on the finite element analysis, the following conclusions can be drawn from this study:

The height and geometry of the arch was found to be considerably influenced by the piles' location and deflection in the embankment.

The height of the arching zone is increased by the increase of the pile spacing for a fixed fill height.

The main reason for the increased K value near the toe compared to the centerline is the inclined nature of the loads at the sloped part under the fill's shoulders not the arching behavior.

The principal stress directions successfully captured the distinct arch geometries at the embankment center, shoulders, and toes.

ACKNOWLEDGMENT

The authors would like to thank the Scientific and Research Council of Turkey (TUBITAK) for supporting this study with project number 122M040.

REFERENCES

Burland, J. B. (1965). The yielding and dilation of clay. correspondence, Géotechnique, 15(1), 211-214.

Chen, R. P., Liu, Q. W., Wu, H. N., Wang, H. L., and Meng, F. Y. (2020). Effect of particle shape on the development of 2D soil arching. Computers and Geotechnics, 125, 103662.

Fagundes, D. F., Almeida, M. S., Thorel, L., and Blanc, M. (2017). Load transfer mechanism and deformation of reinforced piled embankments. Geotextiles and Geomembranes, 45(2), 1-10.

Han, J., Bhandari, A., and Wang, F. (2012). DEM analysis of stresses and deformations of geogrid-reinforced embankments over piles. International Journal of geomechanics, 12(4), 340-350.

Han, J., and Gabr, M. A. (2002). Numerical analysis of geosynthetic-reinforced and pile-supported earth platforms over soft soil. Journal of geotechnical and geoenvironmental engineering, 128(1), 44-53.

Hewlett, W. J., and Randolph, M. F. (1988). Analysis of piled embankments. In International journal of rock mechanics and mining sciences and geomechanics abstracts (Vol. 25, No. 6, pp. 297-298). Elsevier Science.

Hird, C. C., Pyrah, I. C., Russell, D., and Cinicioglu, F. J. C. G. J. (1995). Modelling the effect of vertical drains in two-dimensional finite element analyses of embankments on soft ground. Canadian Geotechnical Journal, 32(5), 795-807.

Indraratna, B., Sathananthan, I., Bamunawita, C., and Balasubramaniam, A. S. (2005). Theoretical and numerical perspectives and field observations for the design and performance evaluation of embankments constructed on soft marine clay. In Elsevier geo-engineering book series (Vol. 3, pp. 51-89). Elsevier.

Jenck, O., Dias, D., and Kastner, R. (2007). Two-dimensional physical and numerical modeling of a pile-supported earth platform over soft soil. Journal of Geotechnical and Geoenvironmental Engineering, 133(3), 295-305.

Karthigeyan, S., Ramakrishna, V. V. G. S. T., and Rajagopal, K. (2007). Numerical investigation of the effect of vertical load on the lateral response of piles. Journal of Geotechnical and Geoenvironmental Engineering, 133(5), 512-521.

Kelesoglu, M. K., and Cinicioglu, S. F. (2010). Free-field measurements to disclose lateral reaction mechanism of piles subjected to soil movements. Journal of geotechnical and geoenvironmental engineering, 136(2), 331-343.

King, D. J., Bouazza, A., Gniel, J. R., Rowe, R. K., and Bui, H. H. (2017). Load-transfer platform behaviour in embankments supported on semi-rigid columns: implications of the ground reaction curve. Canadian Geotechnical Journal, 54(8), 1158-1175.

Lai, H. J., Zheng, J. J., Cui, M. J., and Chu, J. (2020). "Soil arching" for piled embankments: insights from stress redistribution behaviour of DEM modelling. Acta Geotechnica, 15, 2117-2136.

Lai, H. J., Zheng, J. J., Zhang, J., Zhang, R. J., and Cui, L. (2014). DEM analysis of "soil"-arching within geogrid-reinforced and unreinforced pile-supported embankments. Computers and Geotechnics, 61, 13-23.

Lai, H. J., Zheng, J. J., Zhang, R. J., and Cui, M. J. (2016). Visualization of the formation and features of soil arching within a piled embankment by discrete element method simulation. Journal of Zhejiang University-SCIENCE A, 17(10), 803-817.

Lai, H. J., Zheng, J. J., Zhang, R. J., and Cui, M. J. (2018). Classification and characteristics of soil arching structures in pile-supported embankments. Computers and Geotechnics, 98, 153-171.

Low, B. K., Tang, S. K., and Choa, V. (1994). Arching in piled embankments. Journal of geotechnical engineering, 120(11), 1917-1938.

Meena, N. K., Nimbalkar, S., Fatahi, B., and Yang, G. (2020). Effects of soil arching on behavior of pile-supported railway embankment: 2D FEM approach. Computers and Geotechnics, 123, 103601.

Mesri, G., and Choi, Y. K. (1985). Settlement analysis of embankments on soft clays. Journal of Geotechnical Engineering, 111(4), 441-464.

Mesri, G., Lo, D. O. K., and Feng, T. W. (1994, January). Settlement of embankments on soft clays. In Proceedings of the Conference on Vertical and Horizontal Deformations of Foundations and Embankments. Part 2 (of 2) (pp. 8-56). Publ by ASCE.

Nunez, M. A., Briançon, L., and Dias, D. C. F. S. (2013). Analyses of a pile-supported embankment over soft clay: Full-scale experiment, analytical and numerical approaches. Engineering Geology, 153, 53-67.

Oztoprak, S., and Cinicioglu, S. F. (2005). Soil behaviour through field instrumentation. Canadian geotechnical journal, 42(2), 475-490.

Oztoprak, S., and Cinicioglu, S. F. (2007). Looking into an appropriate methodology for the embankment design and construction on soft soils. Lowland Technology International, 9(2, Dec), 21-28.

Oser, C., and Cinicioglu, S. F. (2017). Embankment Design Method Combining Limit-State Approach with Stress-Path Application. International Journal of Geomechanics, 17(4), 04016101.

Terzaghi, K. 1943. "Theoretical soil mechanics," John Wiley and Sons, New York, 11-15.

Van Eekelen, S. J. M., Bezuijen, A., and Van Tol, A. F. (2013). An analytical model for arching in piled embankments. Geotextiles and Geomembranes, 39, 78-102.

Van Eekelen, S. J. M., and Han, J. (2020). Geosynthetic-reinforced pile-supported embankments: state of the art. Geosynthetics International, 27(2), 112-141.

Zheng, G., Yang, X., Zhou, H., and Chai, J. (2019). Numerical modeling of progressive failure of rigid piles under embankment load. Canadian Geotechnical Journal, 56(1), 23-34.